SCIENTIFIC REPORTS

OPEN

SUBJECT AREAS:
PRE-CLINICAL STUDIES
AUTOINFLAMMATORY SYNDROME

Received
5 February 2014

Accepted
22 May 2014

Published
18 June 2014

Correspondence and requests for materials should be addressed to U.A.W. (ulrich.walker@usb.ch)

* These authors contributed equally to this work.

Time-dependent and somatically acquired mitochondrial DNA mutagenesis and respiratory chain dysfunction in a scleroderma model of lung fibrosis

Amiq Gazdhar[1,2]*, Dirk Lebrecht[3]*, Michael Roth[4], Michael Tamm[4], Nils Venhoff[3], Chingching Foocharoen[5], Thomas Geiser[1,2] & Ulrich A. Walker[3,6]

[1]Dept. of Pulmonary Medicine University Hospital Bern, Bern Switzerland, [2]Dept. of Clinical Research, University of Bern, Bern Switzerland, [3]Dept. of Rheumatology & Clinical Immunology, University Hospital Freiburg, Freiburg, Germany, [4]Pulmonary Cell Research, Biomedicine, University Basel; Pneumology, Internal Medicine, University Hospital Basel, Switzerland, [5]Division of Rheumatology, Dept. of Medicine, Khon Kaen University, Khon Kaen, Thailand, [6]Dept. of Rheumatology at Basel University, Basel, Switzerland.

Reactive oxygen species (ROS) have been implemented in the etiology of pulmonary fibrosis (PF) in systemic sclerosis. In the bleomycin model, we evaluated the role of acquired mutations in mitochondrial DNA (mtDNA) and respiratory chain defects as a trigger of ROS formation and fibrogenesis. Adult male Wistar rats received a single intratracheal instillation of bleomycin and their lungs were examined at different time points. Ashcroft scores, collagen and TGFβ1 levels documented a delayed onset of PF by day 14. In contrast, increased malon dialdehyde as a marker of ROS formation was detectable as early as 24 hours after bleomycin instillation and continued to increase. At day 7, lung tissue acquired significant amounts of mtDNA deletions, translating into a significant dysfunction of mtDNA-encoded, but not nucleus-encoded respiratory chain subunits. mtDNA deletions and markers of mtDNA-encoded respiratory chain dysfunction significantly correlated with pulmonary TGFβ1 concentrations and predicted PF in a multivariate model.

Scleroderma (also called systemic sclerosis, SSc) is a disease in which interstitial lung involvement represents the most frequent cause of death[1]. It is believed that pulmonary fibrosis (PF) results from a sequential 'multi-hit' lung injury, after which incomplete alveolar epithelial repair processes foster the release of profibrotic mediators such as transforming growth factor (TGF) β, progressive accumulation of excess extracellular matrix, collagen, and scar formation, ultimately leading to architectural distortion[2,3]. Despite some evidence for an involvement of the immune system, the pulmonary collagen deposits are in clinical practice rarely amenable to immunosuppressive therapy and many patients have remarkably little evidence of cellular inflammation in the pulmonary parenchyma[4,5].

The exact initial triggers of the lung injury are not known but several lines of evidence point towards an important role of reactive oxygen species (ROS). ROS were found at great abundance early in the disease process[6,7] and were found to be constitutively produced by fibroblasts; conversely ROS enhance fibroblast proliferation and collagen formation[8]. The mechanism that perpetuates the production of superoxide and hydrogen peroxide in SSc fibroblasts is not understood but it is intracellular and independent of cytokines[8]. ROS also activate latent TGFβ1, which in turn fosters the production of more ROS[9–11]. This intrinsic TGFβ1 cycle also promotes the epithelial mesenchymal transition (EMT), a process in which pulmonary epithelial cells transform to fibroblasts and myofibroblasts[10,12,13]. The importance of ROS in PF is also highlighted by the fact that N-acetylcysteine, a glutathione precursor that inhibits that myofibroblast formation[14], attenuated PF in an animal model[15] and in combination with other drugs - the decline of lung function in a randomized trial of patients with idiopathic PF[16]. Up to now. the exact role of oxidant stress in the pathogenesis of human PF remains unclear, and the use of anti-

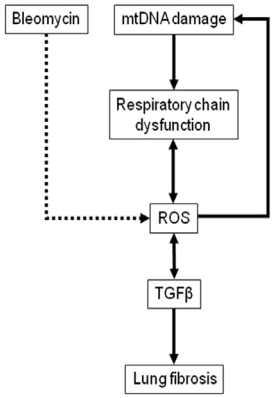

Figure 1 | Simplified hypothesis of mitochondrial involvement in the pathogenesis of bleomycin induced PF. Bleomycin induces ROS that are perpetuated by positive feedback loops involving respiratory impairment and mitochondrial mutagenesis. ROS, respiratory chain dysfunction, or a combination of both, then induce TGFβ1 and interstitial lung disease[3,10].

oxidants controversial. An ongoing clinical comparison of N-acetylcysteine alone and matching placebo will help to shed more light on the therapeutic role of this antioxidant in patients with idiopathic PF[17].

Mitochondria may be involved in the pathogenesis of PF because on the one hand, they are the main cellular producers of ROS and on the other hand are themselves subject to oxidative injury of their lipids, protein structures and genome (e.g. mitochondrial DNA, mtDNA). In this study, we investigate the specific hypothesis that mutations in mtDNA accumulate with time during the progression of PF and contribute to, or may even be an important driver of ROS production and subsequent fibrosis. Our hypothesis hinges on the fact that unopposed mtDNA mutagenesis interferes with mitochondrial transcription and respiratory chain protein synthesis, a process which augments the liberation of ROS, which then either attack the respiratory chain itself, or in turn damage mtDNA[18]. ROS may therefore close vicious circles of interconnected mtDNA and respiratory chain insults. Such vicious circles may continue to operate even in the absence of the inciting event and since mitochondrial ROS are also potent activators of TGFβ1[10,16] then account for the relentless progression of PF (figure 1)[8].

In this study, we investigated the hypothesis of somatically acquired lesions in mitochondria as possible perpetuators of the relentless disease process by investigating mtDNA mutations and their association with interstitial lung disease in a bleomycin model of PF[19]. We chose the bleomycin model because (i) bleomycin induces ROS, (ii) high doses of bleomycin frequently induce PF in humans and (iii) the development of SSc-like skin fibrosis has been observed in patients treated with bleomycin[20].

Results

Delayed onset of bleomycin lung injury. The pulmonary collagen content measured by means of the hydroxyproline assay increased with time. From a mean of 113 μg/mg wet tissue (SD 74) in the group not treated with bleomycin (control rats), the mean pulmonary hydroxyproline content increased by 154% after 48 hours ($p = 0.08$.), 169% after 7 days ($p = 0.016$), and 167% after 14 days ($p = 0.01$). Similarly, in the control animals, the median Ashcroft score was 1.2 (interquartile range (IQR) 1.0, 1.6). At 24 hours and 48 hours after bleomycin instillation, the Ashcroft score remained unchanged with median scores of 1.1 and 1.2, respectively. The Ashcroft score increased 7 days after bleomycin instillation with a median Ashcroft score of 1.8, (IQR 1.4, 2.2, $p = 0.053$, Table 1) but only at the 14 day time point, the Ashcroft score differed significantly from control values (median 2.5, IQR 2.0, 3.1), $p = 0.014$, Table 1). As expected, the Ashcroft score and the results from the hydroxyproline assay correlated ($r = 0.41$, $p = 0.004$).

Taken together, the results demonstrate that the development of PF was time dependent and significantly established not before one to two weeks after bleomycin instillation.

α-SMA immunoreactivity was detected in normal lungs, only in the trachea and smooth muscle cells of the pulmonary blood vessels and no significant changes were observed 24 hours post bleomycin instillation. While a few immunoreactive cells were observed at 48 hours, larger areas of α-SMA immunoreactivity were observed in the thickened interstitial space after 7 days, increasing in number and size at day 14 after bleomycin injury (Figure 2). These data confirm the presence of myofibroblasts in the fibrotic scar.

Delayed increase of pulmonary TGFβ1 formation. Similar to the onset of PF, the levels of pulmonary TGFβ1 as a key profibrotic cytokine showed an increase with time (Table1). The median pulmonary TGFβ1 content increased from baseline (2.27 ng/ml, IQR 1.76, 2.48) but was significantly different from control lungs only at day 14 (2.86 ng/ml (IQR 2.76, 2.99, $p < 0.001$). TGFβ1 levels significantly correlated with the increased collagen content ($r = 0.44$, $p = 0.002$) and coincided with the deteriorating Ashcroft score.

ROS are formed early and increase with time. MDA levels as an indirect indicator of the formation of ROS were elevated in the lung early after bleomycin administration (Table 1). Even after 24 hours, the median MDA levels were augmented ($p = 0.02$); MDA then continued to increase progressively and the highest MDA levels were measured 14 days after bleomycin instillation ($p < 0.001$, Table 1). MDA levels were also loosely, but significantly correlated with the pulmonary collagen content ($r = 0.3$, $p = 0.03$) and with TGFβ1 concentrations ($r = 0.30$, $p = 0.02$).

Table 1 | Effects of bleomycin on lung mitochondria. * $p < 0.001$ vs. 0 hours; † $p < 0.05$ vs. 0 hours

Time after intratracheal bleomycin	0 hours	24 hours	48 hours	7days	14 days
Number of rats examined	10	10	9	10	10
Ashcroft score, median (IQR)	1.2 (1.0, 1.6)	1.1 (1.0, 1.2)	1.2 (1.0, 1.7)	1.8 (1.4, 2.2)	2.5 (2.0, 3.1)†
Collagen (μg/mg wet tissue), mean (SD)	113 (74)	30 (9)†	174 (70)	192 (58)†	189 (37)†
TGFβ1 (ng/ml), median (IQR)	2.27 (1.76, 2.48)	2.09 (1.97, 2.24)	2.60 (2.07, 2.95)	2.41 (2.19, 2.75)	2.86 (2.76, 2.99)*
Malon dialdehyde (μmol/g lung), median (IQR)	29 (21, 43)	64 (53, 70)†	89 (84, 98)†	102 (91, 146)*	125 (106, 221)*
Total mtDNA copy number/cell, mean (SD) ((mean(m(mean copies/cell)	59 (10)	65 (21)	58 (11)	64 (20)	50 (10)†
Common deletion (% of total mtDNA), median (IQR)	0 (0, 17)	0 (0, 7)	0 (0, 21)	30 (20, 44)†	47 (42, 54)*
COX-activity (μmoles min^{-1} g $protein^{-1}$), mean (SD)	1.7 (1.8)	0.8 (0.4)	2.0 (2.3)	0.9 (1.0)	0.3 (0.2)*
COX/SDH-ratio, mean (SD)	1.8 (1.9)	1.5 (1.9)	1.0 (1.0)	0.6 (0.8)†	0.1 (0.1)*
COXI/COXIV-ratio (% of control), mean (SD)	100 (20)	132 (28)†	63 (16)*	76 (30)†	59 (11)*
COXIV/GAPDH-ratio (% of control), mean (SD)	100 (22)	80 (18)	100 (20)	101 (23)	97 (6)

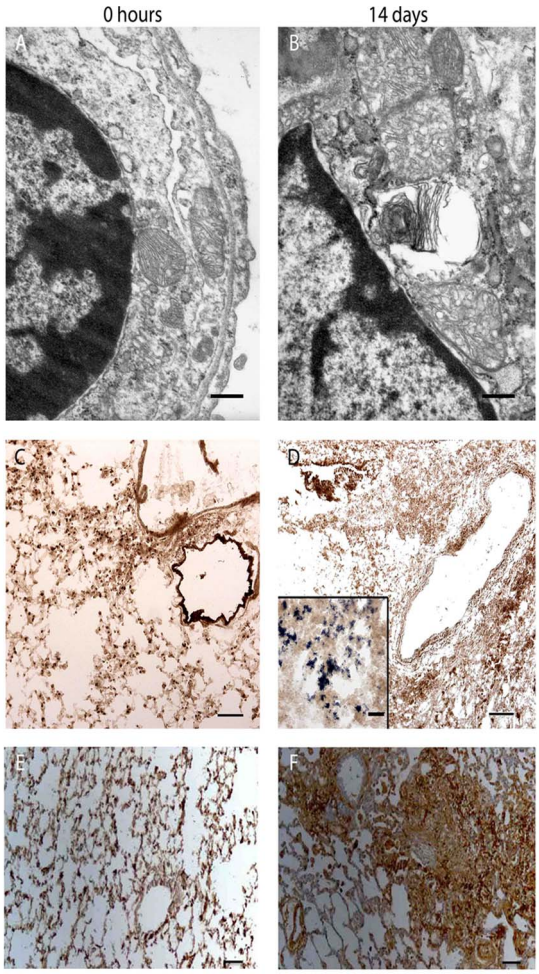

Figure 2 | Effects of bleomycin on lung histology. Representative electron micrographs (A, B) demonstrate mitochondrial enlargement, disrupted crystal architecture and intracytoplasmic vacuoles in an alveolar epithelial cell at day 14. Panels C and D demonstrate depressed COX activity in pulmonary tissue at day 14 (brown stain in COX/SDH histochemistry) and an upregulation of SDH activity (blue stain) not visible at day 0 (insert in panel D). Panels E and F show the expression of αSMA. In normal lung, brown staining was only observed in the smooth muscle around the airways (E); a representative slide of lung tissue 14 days after bleomycin however documents excess αSMA expression in the thickened interstitial space (F). Magnification bars: 4 μm (A,B), 40 μm (C,D, insert D); 100 μm (E,F).

These data demonstrate that ROS formation occurs early after the instillation of bleomycin, continues to increase in the absence of further bleomycin applications, and precedes the development of PF.

mtDNA mutagenesis coincides with the onset of PF. The mean pulmonary copy numbers of total mtDNA remained unchanged compared to controls at 24 hour, 48 hour and 7 day time points (Table 1). Fourteen days after the bleomycin instillation however, the mtDNA copy numbers were significantly reduced compared to controls (mean wild type mtDNA levels 84% of control values, $p = 0.046$).

The 'common' mtDNA deletion was only detected at low levels in control lungs and at the early time points after bleomycin exposure (Table 1). Six control animals, eight animals at the 24 hour time point and six animals at the 48 hour time point did not have any detectable deletion. In contrast, the 'common' deletion was detected in all rats after 7 and 14 days, when also high proportions of mtDNA molecules were detected (median percentage of deleted among total mtDNA molecules 30%, $p = 0.006$ and 47%, $p < 0.001$, respectively vs. 0% in controls).

Among all rat lungs, the proportions of deleted mtDNA molecules positively correlated with the degree of PF as assessed by Ashcroft score ($r = 0.48$, $p < 0.001$, figure 3), pulmonary collagen content ($r = 0.26$, $p < 0.001$), and TGFβ1 levels ($r = 0.57$, $p < 0.001$, figure 3). These data indicate that the accumulation of significant amounts of mtDNA mutations coincides with the onset of PF.

Delayed onset of mtDNA-encoded respiratory chain dysfunction. We measured the activity of COX, a mitochondrial respiratory chain enzyme whose subunits are encoded in part by mtDNA and in part by nDNA. Fourteen days after bleomycin injury, the ratio of COX activity/wet tissue was significantly reduced ($p < 0.02$) with only 17.6% of control activity remaining (Table 1).

We then normalized COX activity for the activity of SDH, a respiratory chain enzyme that is exclusively encoded by nDNA. In the lungs the resulting mean COX/SDH-ratio was 1.8 in control rats and decreased progressively to 83%, 57%, 33% and 6%, at 24 hours, 48 hours, 7 days and 14 days (Table 1). This progressive loss of mtDNA-encoded respiratory chain activity also highly correlated with the frequency of the mtDNA common deletion ($r = -0.37$, $p = 0.007$) and with TGFβ1 levels $r = 0.57$, $p < 0.001$). COX histochemistry confirmed the downregulation of COX-activity, although a particular cell type accounting for this effect could not be observed (Figure 2).

We then analyzed the subunit composition of COX by means of Western Blots and normalized the expression of the mtDNA encoded COX subunit I for that of the simultaneously probed nDNA-encoded COX subunit IV. The mean COXI/COXIV-ratio was increased in the rats at 24 hours (132% compared to controls), but was substantially reduced at 48 hours, 7 days and 14 days after bleomycin exposure (mean COXI/COXIV-ratio 63%, 76% and 60% of control values (Table 1). Furthermore, the COXI/COXIV-ratio was negatively correlated with the collagen content in the lungs ($r = -0.57$, $p < 0.001$), the pulmonary TGFβ1 content ($r = -0.58$, $p < 0.001$), the pulmonary concentrations of MDA ($r = -0.30$, $p = 0.035$), and the frequency of mtDNA deletions ($r = -0.36$, $p = 0.01$).

By means of Western blot, we lastly quantified the presence of the COXIV subunit by normalizing the COXIV signal to that of the simultaneously probed GAPDH protein in lung tissue. The resulting COXIV/GAPDH-ratio is an indicator of the expression of nDNA-encoded respiratory chain components but did not statistically differ between time points and did not correlate with both markers of PF and TGFβ1 concentrations in the lung.

These results indicate that the reduced mitochondrial respiratory chain activity is highly correlated with markers of PF and can be attributed to a defect in the mtDNA-encoded, but not to nDNA-encoded COX subunits whereas the expression of nDNA-encoded respiratory chain components is entirely preserved.

Electron microscopy of lung tissue at day 14 (Figure 2) revealed a pronounced enlargement and a disrupted architecture of pulmonary mitochondria, similar to that seen in other mitochondrial disorders [28]. Less pronounced, but similar ultrastructural abnormalities of the mitochondria were also seen at day 7, but not at earlier time points.

Multivariate analysis of parameters associated with PF. Finally, we identified independent predictors of Ashcroft scores, pulmonary hydroxyproline and TGFβ1 content in a multivariate median regression analysis (Table 2). This analysis confirms acquired mtDNA deletions and markers of respiratory chain dysfunction, underscoring the association of mtDNA mutagenesis and mtDNA-encoded respiratory defect with the delayed acquisition of PF.

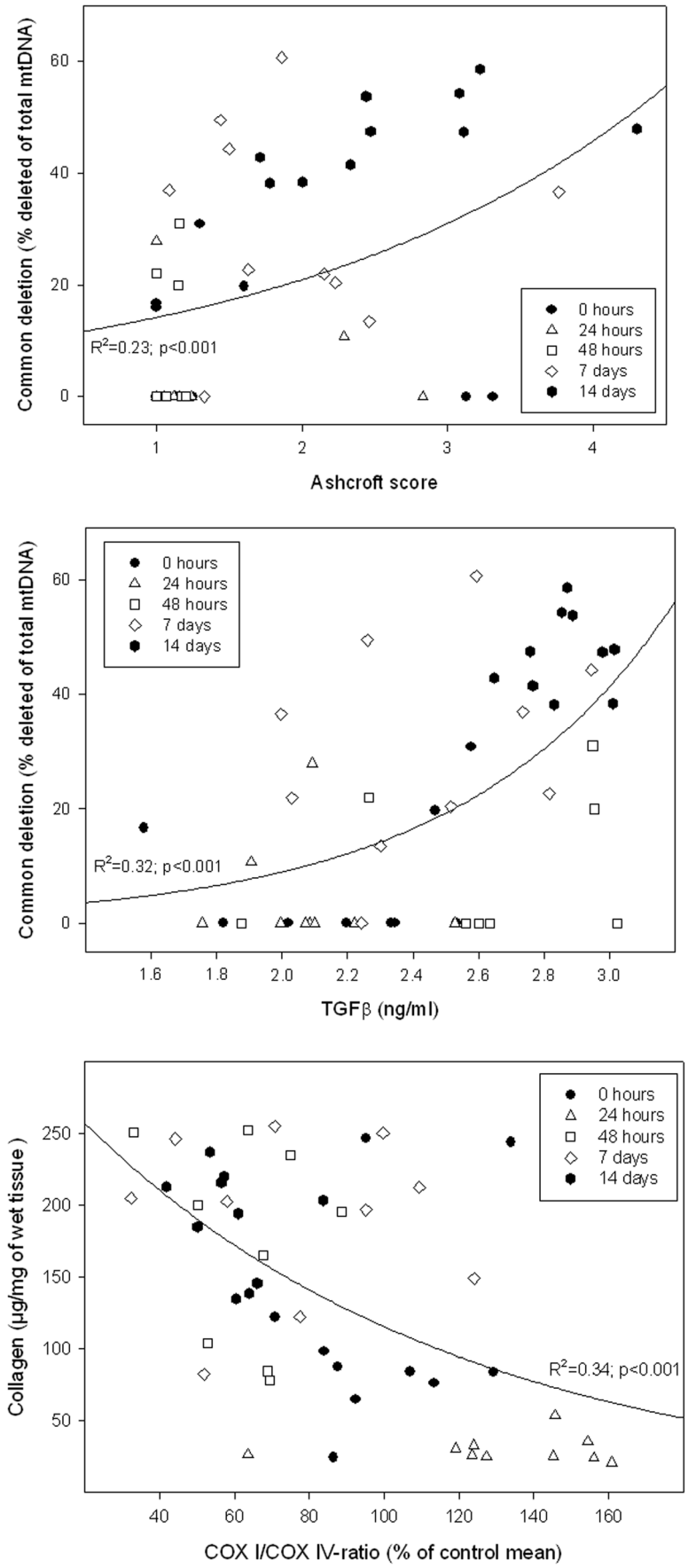

Figure 3 | **Correlations between PF, pulmonary TGFβ1 content, mitochondrial mutagenesis and mitochondrial function.**

Table 2 | Acquired mtDNA mutations and respiratory chain dysfunction as independent predictors of Ashcroft scores, pulmonary collagen deposition (hydroxyproline), and the proinflammatory cytokine TGFβ1. Significant p-values were calculated in a multivariate median regression analysis; non-significant variables are presented as empty cells

Variable	Ashcroft score	Hydroxyproline concentration	TGFβ1 concentration
Total mtDNA copy numbers/lung cell			
Common mtDNA deletion (% of total mtDNA)	0.004	0.02	0.003
Malon dialdehyde concentration			
COX-activity		0.01	0.005
COX/SDH-ratio			
COXI/COXIV-ratio		0.03	<0.001

Discussion

The aim of this study was to investigate the role of somatically acquired mitochondrial dysfunction in the irreversible perpetuation of PF in a rat lung fibrosis model. We demonstrate that a single instillation of bleomycin induces ROS formation with early functional and genetic mitochondrial lesions and that these mitochondrial defects are perpetuated and augmented with time in the absence of additional bleomycin dosing. It is known that quantitative and qualitative mtDNA-defects must exceed a threshold in order to achieve pathogenic relevance[21], possibly accounting for the onset of fibrotic activity at later stages.

Importantly, our data indicate that the respiratory impairment is associated with selective impairment of mitochondrial, but not nuclear encoded respiratory chain subunits. ROS also impair the function of polymerase-gamma, the enzyme responsible for mtDNA replication. This fact may account at least in part for the decrease in total mtDNA levels observed at day 14 and contribute to the functional defect in the expression of mtDNA encoded respiratory chain subunits.

An aberrant response to recurrent insults is now accepted as an important mechanism in the etiology of PF[2,3]. There is ample evidence suggesting that ROS are generated in the pulmonary parenchyma and play a vital role in fibrotic process[6,7,9]. Bleomycin releases large amounts of ROS[22–25] which are important in the onset of PF in this model, as highlighted by the fact that the absence of ROS is protective[26].

In the current study we demonstrate that marked mitochondrial impairment is a likely significant source of ROS and its profibrotic mechanism. Furthermore, interconnected and via ROS-formation self-perpetuating and self-augmenting mtDNA and respiratory chain insults could explain the relentless progression and delayed onset of PF[8]. It is however still not fully understood, if mitochondrial damage also promotes PF through mechanisms other than ROS-formation and subsequent activation of TGFβ1[10,27], for example by directly triggering apoptotic pathways in the lung parenchyma[28].

The mitochondrial theory of ageing associates oxidative stress with mitochondrial mutagenesis and respiratory dysfunction of organs at senescence[29,30]. Our data therefore provide an explanation for the so far elusive link between ageing as perhaps the strongest non-environmental risk factor for interstitial lung involvement and the onset of PF in non SSc patients[3,31]. Such mitochondrial impairment has been demonstrated in models of liver fibrosis and there is growing interest in the potential role of acquired mtDNA mutations in other late-onset diseases[30].

Mitochondria participate in cold-induced vasospasm (Raynaud's phenomenon), a symptom that is present in virtually every SSc patient[32,33]. In Raynaud's phenomenon, mitochondria generate ROS in vascular smooth muscle cells which then augment vasoconstriction by mobilizing adrenoceptors to the cell surface via the RhoA/Rho kinase (ROCK) pathway[32–34]. It is therefore interesting to speculate if the pathogenetic mechanisms that operate in SSc are associated with mitochondrial damage in other organ systems.

We have to acknowledge, that our results, although compelling, do not provide causal proof of the pathogenetic role of mitochondrial dysfunction in lung injury. Recent data however found a suppressed synthesis of alveolar ATP and mitochondrial dysfunction in an *in vivo* model of acute lung injury and even more importantly, it was demonstrated that the experimental normalization of mitochondrial bioenergetics was protective[35].

We do not know which cell types account for our findings. Fibroblasts are a possible candidate, because when explanted from fibrotic lungs after bleomycin treatment these cell types retain their profibrotic phenotype in culture[36], in support of an intracellular defect which is possibly fixed in the mitochondrial genome. In our study, we analyzed the respiratory chain activity by means of histochemistry but were not able to demonstrate the specific involvement of a particular cell type. This finding was strengthened by electron microscopy which revealed ultrastructural damage of mitochondria in a variety of pulmonary cells, including alveolar epithelial cells. Alveolar epithelial cells may also provide a source of ROS, as they have been shown to be subject to mtDNA injury and consecutive apoptosis[37]. Failure of alveolar epithelial cells to reepithealize in response to injury is an important mechanism in the pathogenesis of PF.

It is therefore likely, that several cell types account for our findings. Current studies from our group now determine the presence and functional relevance of mtDNA mutagenesis in lung biopsies from patients with PF. Additional *in vitro* studies using fibroblasts devoid of any mtDNA[38] will help to elucidate the effect of mitochondrial lesions on the response of lung fibroblasts to profibrotic stimuli. Our findings may also help in the rational development of protective ROS scavengers.

Conclusions

Our data suggest that mtDNA alterations and respiratory chain defects, initiated during acute bleomycin exposure, and gradually accumulating over time could represent an important factor in the delayed onset of PF and in the perpetuation of ROS-mediated lung injury.

Methods

Animals. Fifty adult male Wistar rats (220–240 g) were obtained from the animal care facility in Bern, Switzerland. Experiments were performed in accordance to the standards of the European Convention of Animal Care. The study protocol was approved by the University of Bern Animal Study Committee.

Instillation of bleomycin. At day one of the protocol, rats were anesthetized by inhalation of 4% isoflurane, intubated with a 14 gauge catheter (Insyte, Madrid, Spain) and instilled intratracheally with bleomycin (1.28 U/rat) to both lungs. The dosage of bleomycin was based on preliminary experiments showing induction of PF with lowest mortality[39]. Animals were sacrificed in groups of ten 24 hours, 48 hours, 7 days, or 14 days after intratracheal bleomycin instillation. Lung aliquots were either fixed in formalin or snap frozen for further analysis. Ten rats with no bleomycin instillation served as controls. One rat in the 48 hour group was found dead 24 hours after bleomycin instillation; therefore the 48 hour group had 9 animals available for the analysis, whereas all other groups had 10 rats each.

Histology and Ashcroft scoring. The extent of PF was evaluated with the Ashcroft score on formalin-fixed sections after haematoxylin and eosin staining of the mid apical regions of the left and the middle lobes of the right lungs[40]. The pathologist was blinded to the group status of the specimen. Five microscopic fields were randomly chosen and a score ranging from 0 (normal) to 8 (total fibrosis) was given to each field. For each animal the mean score of all fields was calculated.

Hydroxyproline Assay. Lung collagen content was quantified by means of the hydroxyproline assay as described[39]. Frozen middle regions of both lungs where

weighted and homogenized. The homogenate was treated with 10% trichloroacetic acid, hydrolyzed with 6 M HCl (18 hours, 110°C) and adjusted to pH 7.0 with NaOH. Oxidation was initiated by incubation with 1 ml of chloramine T-reagent (20 minutes, room temperature) and stopped by addition of 1 ml of 3.15 M $HClO_4$. After incubation with Ehrlich reagent (p-dimethylaminobenzaldehyde added to methyl cellosolve) for 20 minutes at 55-65°C the absorbance of each sample was measured at 557 nm. A standard curve was generated using known concentrations of hydroxyproline. All chemicals were obtained from Sigma Aldrich, USA.

Electron microscopy. The lungs of two randomly selected rats from each group were examined by electron microscopy. Aliquots were post-fixed in OsO_4 (1%), dehydrated and embedded in Epon[41]. Ultra thin sections were stained with lead citrate and uranyl acetate and viewed in a Zeiss electron microscope (EM 900) operated at 50 kV.

ROS formation. Malondialdehyde (MDA) is one of the end products of lipid peroxidation and an indicator of ROS production and oxidative stress. MDA was spectrophotometrically quantified in tissues with an assay for thiobarbituric acid reactive material, as described elsewhere[41].

Measurement of TGFβ1 levels in lung homogenate. Lung protein was extracted using a lysis buffer containing PBS, Nonidet P-40 (1%), EDTA (100 mM), and pepstatin A (1 μg/ml) and TGFβ1 levels measured using an ELISA kit (R&D Systems, Abingdon, U.K)[39].

Anti α-smooth muscle actin immunohistochemistry. Formaline fixed sections were deparaffinised in xylene series and rehydrated in decreasing ethanol series. Slides were pre-treated by microwave in citrate buffer (100 mM, pH 7.0) for 10 minutes, washed three times with Tris-buffered saline containing 0.1% tween and incubated overnight at 4°C with an anti α-smooth muscle actin (α-SMA) antibody (1 : 100, Sigma Aldrich, USA). Antibody binding was detected as a brown stain by means of a peroxidase system and 3,3′-diaminobenzidine as a substrate (EnVision and System HRP DAB, Dako USA).

MtDNA-content. Total DNA was extracted with the QIAamp DNA isolation kit (Qiagen, Hilden, Germany). MtDNA and nDNA copy numbers were determined by quantitative polymerase chain reaction (PCR) using LightCycler® 480 Real-Time PCR System (Roche, Mannheim, Germany) on a 384 well plate. 10 μl reactions contained 5 μl of SYBR Green I Master mix (Roche, Mannheim, Germany), 10 ng DNA template and 0.5 μM of each primer. The mtDNA was amplified between nucleotide positions 2469 and 2542 with the forward primer, 5′-AAT GGT TCG TTT GTT CAA CGA TT-3′ and the backward primer 5′-AGA AAC CGA CCT GGA TTG CTC-3′. For the detection of nuclear DNA (nDNA) we selected GAPDH between nucleotide positions 494 and 671, using the forward primer 5′-TGC ACC ACC AAC TGC TTA G-3′ and the backward primer 5′-GGA TGC AGG GAT GAT GTT C-3′. Amplifications of mitochondrial and nuclear products were separately performed as triplicates, with the following conditions: an pre-incubation at 95°C for 5 min, was followed by 40 cycles of a 3 steps amplification (95°C, 10 sec; 50°C 10 sec; 72°C 15 sec) ending with a melting curve for PCR product identification (95°C, 5 sec; 65°C, 1 min). Absolute mtDNA and nDNA copy numbers were calculated using serial dilutions of plasmids with known copy numbers. The mtDNA copy number per pulmonary cell was calculated as the number of mtDNA copies per two nuclear DNA copies.

Detection and quantification of the common mtDNA-deletion. The mtDNA sequence contains direct repeats between which base pairs may be deleted by slipped mispairing during replication[42,43]. A 4977 base-pair deletion is the most frequent somatically acquired deletion in humans and therefore also termed "common" deletion. We probed for the 4834 base pair rat homologue of the "common" deletion by amplifying 100 ng of genomic DNA with the following extradeletional primers F7825 (5′-TTT CTT CCC AAA CCT TTC CT-3′) and B13117 (5′-AAG CCT GCT AGG ATG CTT C-3′) in a PCR reaction[44]. By choosing a short extension cycle (30 seconds), the deleted molecule was preferentially amplified as a 459 base-pair product. This PCR product was confirmed by sequencing to represent the "common" 4974 base pair mtDNA deletion in rats. The deletion was quantified by densitometry on agarose gels (Quantum ST4v16.03, Vilber Lourmat, Marne-la-Vallee, France) and calibrated with PCR products from templates with known amounts of deleted mtDNA (from cybrids, homoplasmic for the "common" mtDNA-deletion[41,45].

Activity of the mitochondrial respiratory chain. The enzyme activity of cytochrome c-oxidase (COX), a multisubunit respiratory chain complexes which is encoded by nuclear DNA (nDNA) and mtDNA, and succinate dehydrogenase (SDH), which is encoded entirely by nDNA, were measured by spectrophotometry in freshly prepared lung extracts, as described[46].

MtDNA-encoded respiratory chain protein. The subunit I of cytochrome c-oxidase (COXI) is encoded by mtDNA, whereas the subunit IV of cytochrome c-oxidase (COXIV) is encoded by nDNA. The blots were also probed with an antibody (Fitzgerald Industries International Inc., Acton, USA) against glycerol aldehyde phosphate dehydrogenase (GAPDH), an enzyme which is entirely encoded in the nucleus. COXI was quantified by immunoblot densitometry (Quantum ST4v16.03, Vilber Lourmat, Marne-la-Vallee, France) and normalized to the signal of a simultaneously used antibody against COXIV[46].

Statistics. Using Sigma Plot (vs. 12.3) statistical software, repeated measures Analysis of variance (ANOVA) tests were used for between-group comparison, followed by t tests or Wilcoxon-tests s. Linear or non-linear correlations were calculated as appropriate. P values < 0.05 were considered significant. Multivariate median regression analysis was applied to identify factors independently associated with pulmonary collagen content, Ashcroft score, and TGFβ1 levels.

1. Tyndall, A. J. *et al.* Causes and risk factors for death in systemic sclerosis: a study from the EULAR Scleroderma Trials and Research (EUSTAR) database. *Annals of the Rheumatic Diseases* **69**, 1809–1815, doi:10.1136/ard.2009.114264 (2010).
2. Gross, T. J. & Hunninghake, G. W. Idiopathic pulmonary fibrosis. *N Engl J Med* **345**, 517–525, doi:10.1056/NEJMra003200 (2001).
3. King, T. E., Jr., Pardo, A. & Selman, M. Idiopathic pulmonary fibrosis. *Lancet* **378**, 1949–1961, doi:10.1016/S0140-6736(11)60052-4 (2011).
4. Daniels, C. E. *et al.* Imatinib treatment for idiopathic pulmonary fibrosis: Randomized placebo-controlled trial results. *Am J Respir Crit Care Med* **181**, 604–610, doi:10.1164/rccm.200906-0964OC (2010).
5. Tashkin, D. P. *et al.* Cyclophosphamide versus placebo in scleroderma lung disease. *N Engl J Med* **354**, 2655–2666, doi:10.1056/NEJMoa055120 (2006).
6. Cracowski, J. L. *et al.* Enhanced in vivo lipid peroxidation in scleroderma spectrum disorders. *Arthritis Rheum* **44**, 1143–1148, doi:10.1002/1529-0131(200105)44:51143::AID-ANR196>3.0.CO;2-# (2001).
7. Cantin, A. M., North, S. L., Fells, G. A., Hubbard, R. C. & Crystal, R. G. Oxidant-mediated epithelial cell injury in idiopathic pulmonary fibrosis. *J Clin Invest* **79**, 1665–1673, doi:10.1172/JCI113005 (1987).
8. Sambo, P. *et al.* Oxidative stress in scleroderma: maintenance of scleroderma fibroblast phenotype by the constitutive up-regulation of reactive oxygen species generation through the NADPH oxidase complex pathway. *Arthritis Rheum* **44**, 2653–2664 (2001).
9. Cheresh, P., Kim, S. J., Tulasiram, S. & Kamp, D. W. Oxidative stress and pulmonary fibrosis. *Biochim Biophys Acta* **1832**, 1028–1040, doi:10.1016/j.bbadis.2012.11.021 (2013).
10. Koli, K., Myllarniemi, M., Keski-Oja, J. & Kinnula, V. L. Transforming growth factor-beta activation in the lung: focus on fibrosis and reactive oxygen species. *Antioxid Redox Signal* **10**, 333–342, doi:10.1089/ars.2007.1914 (2008).
11. Jain, M. *et al.* Mitochondrial reactive oxygen species regulate transforming growth factor-beta signaling. *J Biol Chem* **288**, 770–777, doi:10.1074/jbc.M112.431973 (2013).
12. Kasai, H., Allen, J. T., Mason, R. M., Kamimura, T. & Zhang, Z. TGF-beta1 induces human alveolar epithelial to mesenchymal cell transition (EMT). *Respir Res* **6**, 56, doi:10.1186/1465-9921-6-56 (2005).
13. Gorowiec, M. R. *et al.* Free radical generation induces epithelial-to-mesenchymal transition in lung epithelium via a TGF-beta1-dependent mechanism. *Free Radic Biol Med* **52**, 1024–1032, doi:10.1016/j.freeradbiomed.2011.12.020 (2012).
14. Felton, V. M., Borok, Z. & Willis, B. C. N-acetylcysteine inhibits alveolar epithelial-mesenchymal transition. *Am J Physiol Lung Cell Mol Physiol* **297**, L805–812, doi:10.1152/ajplung.00009.2009 (2009).
15. Hagiwara, S. I., Ishii, Y. & Kitamura, S. Aerosolized administration of N-acetylcysteine attenuates lung fibrosis induced by bleomycin in mice. *Am J Respir Crit Care Med* **162**, 225–231 (2000).
16. Behr, J. *et al.* Lung function in idiopathic pulmonary fibrosis--extended analyses of the IFIGENIA trial. *Respir Res* **10**, 101, doi:10.1186/1465-9921-10-101 (2009).
17. Raghu, G., Anstrom, K. J., King, T. E., Jr., Lasky, J. A. & Martinez, F. J. Prednisone, azathioprine, and N-acetylcysteine for pulmonary fibrosis. *N Engl J Med* **366**, 1968–1977, doi:10.1056/NEJMoa1113354 (2012).
18. Richter, C. Reactive oxygen and DNA damage in mitochondria. *Mutat Res* **275**, 249-255 (1992).
19. Gazdhar, A. *et al.* Gene transfer of hepatocyte growth factor by electroporation reduces bleomycin-induced lung fibrosis. *Am J Physiol Lung Cell Mol Physiol* **292**, L529–536, doi:10.1152/ajplung.00082.2006 (2007).
20. Beyer, C., Schett, G., Distler, O. & Distler, J. H. Animal models of systemic sclerosis: prospects and limitations. *Arthritis Rheum* **62**, 2831–2844, doi:10.1002/art.27647 (2010).
21. Ambrosio, G. *et al.* Evidence that mitochondrial respiration is a source of potentially toxic oxygen free radicals in intact rabbit hearts subjected to ischemia and reflow. *J Biol Chem* **268**, 18532–18541 (1993).
22. Wallach-Dayan, S. B. *et al.* Bleomycin initiates apoptosis of lung epithelial cells by ROS but not by Fas/FasL pathway. *Am J Physiol Lung Cell Mol Physiol* **290**, L790–L796, doi:10.1152/ajplung.00300.2004 (2006).
23. Phan, S. H., Thrall, R. S. & Ward, P. A. Bleomycin-induced pulmonary fibrosis in rats: biochemical demonstration of increased rate of collagen synthesis. *The American review of respiratory disease* **121**, 501–506 (1980).
24. Doherty, D. E., Hirose, N., Zagarella, L. & Cherniack, R. M. Prolonged monocyte accumulation in the lung during bleomycin-induced pulmonary fibrosis. A noninvasive assessment of monocyte kinetics by scintigraphy. *Lab Invest* **66**, 231–242 (1992).

25. Gao, F., Kinnula, V. L., Myllarniemi, M. & Oury, T. D. Extracellular superoxide dismutase in pulmonary fibrosis. *Antioxid Redox Signal* **10**, 343–354, doi:10.1089/ars.2007.1908 (2008).
26. Manoury, B. *et al*. The absence of reactive oxygen species production protects mice against bleomycin-induced pulmonary fibrosis. *Respir Res* **6**, 11, doi:10.1186/1465-9921-6-11 (2005).
27. Liu, R. M. & Gaston Pravia, K. A. Oxidative stress and glutathione in TGF-beta-mediated fibrogenesis. *Free Radic Biol Med* **48**, 1–15, doi:10.1016/j.freeradbiomed.2009.09.026 (2010).
28. Cheresh, P., Kim, S.-J., Tulasiram, S. & Kamp, D. W. Oxidative stress and pulmonary fibrosis. *Biochimica et Biophysica Acta (BBA) - Molecular Basis of Disease* **12**, S0925–4439, doi:http://dx.doi.org/10.1016/j.bbadis.2012.11.021 (2012).
29. Schon, E. A., DiMauro, S. & Hirano, M. Human mitochondrial DNA: roles of inherited and somatic mutations. *Nat Rev Genet* **13**, 878–890, doi:10.1038/nrg3275 (2012).
30. Faner, R., Rojas, M., Macnee, W. & Agusti, A. Abnormal lung aging in chronic obstructive pulmonary disease and idiopathic pulmonary fibrosis. *Am J Respir Crit Care Med* **186**, 306–313, doi:10.1164/rccm.201202-0282PP (2012).
31. Raghu, G., Weycker, D., Edelsberg, J., Bradford, W. Z. & Oster, G. Incidence and prevalence of idiopathic pulmonary fibrosis. *Am J Respir Crit Care Med* **174**, 810–816, doi:10.1164/rccm.200602-163OC (2006).
32. Bailey, S. R., Mitra, S., Flavahan, S. & Flavahan, N. A. Reactive oxygen species from smooth muscle mitochondria initiate cold-induced constriction of cutaneous arteries. *American journal of physiology. Heart and circulatory physiology* **289**, H243–250, doi:10.1152/ajpheart.01305.2004 (2005).
33. Block, J. A. & Sequeira, W. Raynaud's phenomenon. *Lancet* **357**, 2042–2048, doi:10.1016/S0140-6736(00)05118-7 (2001).
34. Flavahan, N. A. Regulation of vascular reactivity in scleroderma: new insights into Raynaud's phenomenon. *Rheum Dis Clin North Am* **34**, 81–87; vii, doi:10.1016/j.rdc.2007.12.005 (2008).
35. Islam, M. N. *et al*. Mitochondrial transfer from bone-marrow-derived stromal cells to pulmonary alveoli protects against acute lung injury. *Nature medicine* **18**, 759–765, doi:10.1038/nm.2736 (2012).
36. Ponticos, M. *et al*. Pivotal role of connective tissue growth factor in lung fibrosis: MAPK-dependent transcriptional activation of type I collagen. *Arthritis Rheum* **60**, 2142–2155, doi:10.1002/art.24620 (2009).
37. Kim, S. J. *et al*. Mitochondria-targeted Ogg1 and aconitase-2 prevent oxidant-induced mitochondrial DNA damage in alveolar epithelial cells. *J Biol Chem* **289**, 6165–6176, doi:10.1074/jbc.M113.515130 (2014).
38. King, M. P. & Attardi, G. Isolation of human cell lines lacking mitochondrial DNA. *Methods Enzymol* **264**, 304–313 (1996).
39. Gazdhar, A. *et al*. Targeted gene transfer of hepatocyte growth factor to alveolar type II epithelial cells reduces lung fibrosis in rats. *Hum Gene Ther* **24**, 105–116, doi:10.1089/hum.2012.098 (2013).
40. Ashcroft, T., Simpson, J. M. & Timbrell, V. Simple method of estimating severity of pulmonary fibrosis on a numerical scale. *Journal of clinical pathology* **41**, 467–470 (1988).
41. Lebrecht, D., Kokkori, A., Ketelsen, U. P., Setzer, B. & Walker, U. A. Tissue-specific mtDNA lesions and radical-associated mitochondrial dysfunction in human hearts exposed to doxorubicin. *J Pathol* **207**, 436–444, doi:10.1002/path.1863 (2005).
42. Schon, E. A. *et al*. A direct repeat is a hotspot for large-scale deletion of human mitochondrial DNA. *Science* **244**, 346–349 (1989).
43. Samuels, D. C., Schon, E. A. & Chinnery, P. F. Two direct repeats cause most human mtDNA deletions. *Trends Genet* **20**, 393–398, doi:10.1016/j.tig.2004.07.003 (2004).
44. Edris, W., Burgett, B., Stine, O. C. & Filburn, C. R. Detection and quantitation by competitive PCR of an age-associated increase in a 4.8-kb deletion in rat mitochondrial DNA. *Mutat Res* **316**, 69–78 (1994).
45. King, M. P. Use of ethidium bromide to manipulate ratio of mutated and wild-type mitochondrial DNA in cultured cells. *Methods Enzymol* **264**, 339–344 (1996).
46. Lebrecht, D., Setzer, B., Ketelsen, U. P., Haberstroh, J. & Walker, U. A. Time-dependent and tissue-specific accumulation of mtDNA and respiratory chain defects in chronic doxorubicin cardiomyopathy. *Circulation* **108**, 2423–2429, doi:10.1161/01.CIR.0000093196.59829.DF (2003).

Author contributions

A.G. and D.L. (design, experimentation, data collection, interpretation and initial draft of manuscript), N.V. and C.F. (data interpretation and statistical analysis), M.R. and M.T. (design and manuscript corrections) T.G. (design, data interpretation and manuscript corrections), U.A.W. (concept, design, data interpretation, supervision, financial support, initial draft and final approval of the manuscript). This study was founded by the Swiss National Science Foundation.

Additional information

Competing financial interests: The authors declare no competing financial interests.

How to cite this article: Gazdhar, A. *et al*. Time-dependent and somatically acquired mitochondrial DNA mutagenesis and respiratory chain dysfunction in a scleroderma model of lung fibrosis. *Sci. Rep.* **4**, 5336; DOI:10.1038/srep05336 (2014).